Liquid Crystals
Publication details, including instructions for authors and subscription information:
http://www.informaworld.com/smpp/title~content=t713926090

Induction of smectic layering in nematic liquid crystals using immiscible components IV. The effect of bulky lateral carboxyl substituents on the thermotropic behaviour of 2,5-bis[4-(*n*-perfluoroheptyloctyloxy)benzoyloxy]toluene

Coleen Pugh; Aaron C. Small; Carin A. Helfer; Wayne L. Mattice

Online publication date: 06 August 2010

To cite this Article Pugh, Coleen , Small, Aaron C. , Helfer, Carin A. and Mattice, Wayne L.(2001) 'Induction of smectic layering in nematic liquid crystals using immiscible components IV. The effect of bulky lateral carboxyl substituents on the thermotropic behaviour of 2,5-bis[4-(*n*-perfluoroheptyloctyloxy)benzoyloxy]toluene', Liquid Crystals, 28: 7, 991 — 1001

To link to this Article: DOI: 10.1080/02678290110039471

URL: http://dx.doi.org/10.1080/02678290110039471

LIQUID CRYSTALS, 2001, VOL. 28, NO. 7, 991–1001

Induction of smectic layering in nematic liquid crystals using immiscible components IV. The effect of bulky lateral carboxyl substituents on the thermotropic behaviour of 2,5-bis[4-(*n*-perfluoroheptyloctyloxy)benzoyloxy]toluene†

COLEEN PUGH*, AARON C. SMALL, CARIN A. HELFER and WAYNE L. MATTICE

Maurice Morton Institute of Polymer Science, The University of Akron, Akron, Ohio 44325-3909, USA

(*Received 14 September 2000; accepted 28 November 2000*)

Bulky lateral carboxylate substituents were introduced at the benzylic position of 2,5-bis-[4-(*n*-perfluoroheptyloctyloxy)benzoyloxy]toluene by esterification of the corresponding benzyl bromide with potassium carboxylates. In spite of the bulky lateral substituents, none of the 2,5-bis[4-(*n*-perfluoroheptyloctyloxy)benzoyloxy]benzyl carboxylates exhibit a nematic mesophase in addition to, or instead of, the smectic mesophases. All of the crystalline and SmC–SmA transition temperatures and, with the exception of the 9-anthracene carboxylate derivative, all of the isotropization temperatures of the resulting 2,5-bis[4-(*n*-perfluoroheptyl-octyloxy)benzoyloxy]benzyl carboxylates are lower than those of the parent toluene compound. The SmC–SmA transition decreases the most, thereby stabilizing the SmA mesophase. In most cases, the SmC mesophase is destabilized from an enantiotropic to a monotropic mesophase. There is no correlation between any of the transition temperatures and the size of the lateral substituent.

1. Introduction

Although liquid crystals (LCs) were first discovered in 1888 [2], few concepts have been developed for converting between the type of mesophase(s) that they exhibit. One established concept is that lateral substituents can be used to convert smectic mesophases to a nematic mesophase. Lateral substitution at the centre of the mesogen increases the molar volume and decreases the LC packing density [3], thereby hindering their ability to form any kind of liquid crystalline phase if the mesogen is short [4], and smectic mesophases if the mesogen is more extended [4, 5]. For example, 1,4-bis-(4-*n*-octyloxybenzoyloxy)benzene exhibits both a smectic C and a nematic mesophase [6], whereas 2-*n*-alkyl-1,4-bis(4-*n*-octyloxybenzoyloxy)benzenes ($n = 1$–16) exhibit only a nematic mesophase (figure 1) [7]. Figure 1 demonstrates that this lateral substitution also depresses

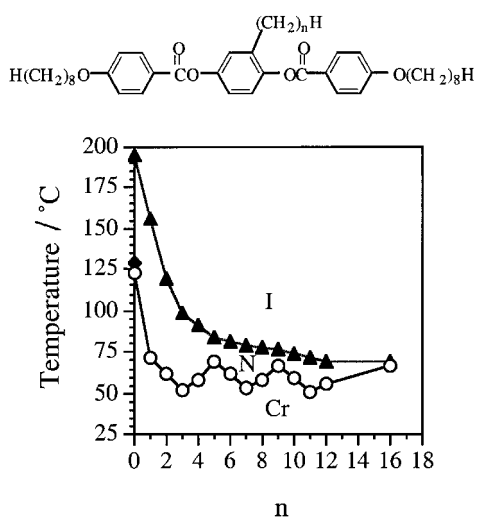

Figure 1. Dependence of the transition temperatures from the crystalline (○), smectic C (◆) and nematic (▲) phases of 2-*n*-alkyl-1,4-bis[4-(*n*-octyloxy)benzoyloxy]benzenes as function of the length of the *n*-alkyl lateral substituent [6, 7].

* Author for correspondence; e-mail: cpugh@polymer.uakron.edu

† For part III see reference [1].

Liquid Crystals ISSN 0267-8292 print/ISSN 1366-5855 online © 2001 Taylor & Francis Ltd
http://www.tandf.co.uk/journals
DOI: 10.1080/02678290110039471

the temperatures of the crystalline melting and nematic–isotropic transitions: both transitions decrease with increasing length of the lateral substituent until they converge to almost constant values.

We recently demonstrated that nematic LCs based on 1,4-bis(4-*n*-alkoxybenzoyloxy)toluene mesogens can be forced to order into smectic layers by terminating their *n*-alkoxy substituents with immiscible fluorocarbon segments [8]. Microsegregation of the hydrocarbon and fluorocarbon segments is apparently so strong that a lateral *n*-alkanoyl substituent is not large enough to disrupt the smectic layering of 2,5-bis[4-(*n*-perfluoroheptyloctyloxy)benzoyloxy]toluene [1]. Instead, the lateral substituent depresses the SmC–SmA transitition temperature more than those of melting and isotropization, thereby stabilizing the SmA mesophase (figure 2). However, long *n*-alkyl and *n*-alkoxy lateral substituents align parallel to the mesogen [9], which enables the molecule to maintain a more rod-like shape and maximize packing. This is consistent with the transition temperatures of the 2,5-bis[4-(*n*-perfluoroheptyloctyloxy)benzoyloxy]benzyl *n*-alkanoates levelling off when the *n*-alkanoyl substituent is at least six carbons long (figure 2).

Because aliphatic hydrocarbons and fluorocarbons have such a strong tendency to microphase separate, LCs containing these segments may offer the most challenging molecules possible for disrupting smectic layering and converting smectic mesophases to a nematic

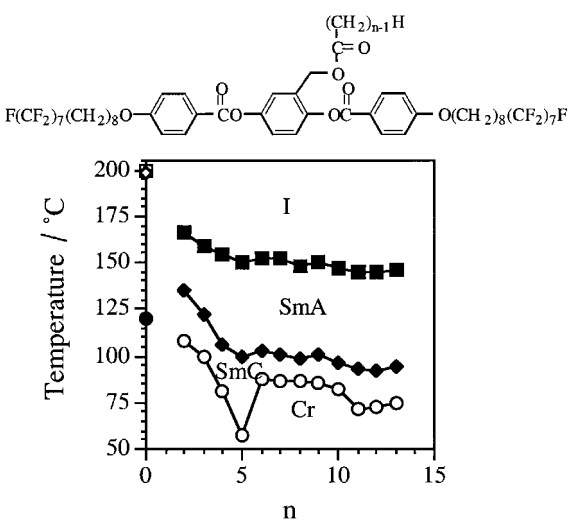

Figure 2. Dependence of the transition temperatures from the crystalline (○), smectic C (◆) and smectic A (■) phases of 2-*n*-alkyl-1,4-bis[4′-(*n*-octyloxy)benzoyloxy]benzenes as a function of the number of carbons in the *n*-alkanoate lateral substituent. The transition temperatures from the crystalline (●), smectic C (◇) and smectic A (□) phases of the unsubstituted 2,5-bis[4-*n*-(perfluoroheptyloctyloxy)-benzoyloxy]toluene are shown at $n = 0$ for comparison [1].

mesophase. Therefore, we are testing the limits of the well established concept that lateral substituents disrupt smectic layering by determining if it is possible to convert the SmC and SmA mesophases of 2,5-bis[4-(*n*-perfluoroheptyloctyloxy)benzoyloxy]toluene (Cr 120 SmC 199 SmA 200 I) into a nematic mesophase by introducing bulkier lateral substituents at its central aromatic ring.

2. Experimental

2.1. *Materials*

1-Adamantanecarboxylic acid (99%), *p*-anisic acid (99%), 9-anthracenecarboxylic acid (99%), 2-ethylbutyric acid (99%), 2-propylpentanoic acid (99%), 3,5-di-*t*-butylenzoic acid (99%) and potassium benzoate (99%) were used as received from Aldrich. 2-Biphenylcarboxylic acid (98%), 4-biphenylcarboxylic acid (98%) and propiolic acid (98%) were used as received from Lancaster. 4-*tert*-Butylbenzoic acid was prepared by hydrolysis of methyl 4-*tert*-butylbenzoate (Aldrich, 99%). 4-Hexadecyloxybenzoic acid and 4-octyloxybenzoic acid were synthesized via Williamson etherification of ethyl-4-hydroxybenzoate with the respective bromoalkane followed by hydrolysis of the ethyl benzoate under basic conditions [10]. Dimethylsulfoxide (DMSO, Fisher) was distilled from CaH_2 under N_2. Reagent grade tetrahydrofuran (THF) was dried by distillation from purple sodium benzophenone ketyl under N_2. 2,5-Bis-[4′-(*n*-perfluoroheptyl octyloxy)benzo yloxy]benzyl bromide was prepared as previously reported [1, 8]. All other reagents and solvents were commercially available and used as received.

2.2. *Techniques*

Unless noted otherwise, all reactions were performed under a N_2 atmosphere. ^{1}H-NMR spectra (δ, ppm) were recorded on a Bruker AM-360 (360 MHz) spectrometer. When necessary, additional peak assignments were made with ^{1}H-^{1}H COSY experiments recorded on a Varian Unity INOVA 400 (400 MHz) spectrometer. All spectra were recorded in $CDCl_3$ with TMS as an internal standard. The thermotropic behaviour of all compounds was determined by a combination of differential scanning calorimetry (DSC) and polarizing optical microscopy (POM). A Perkin-Elmer DSC-7 differential scanning calorimeter was used to determine the thermal transitions at 10°C min^{-1}. The endothermic and exothermic peaks were read at their maximum and minimum energies, respectively. Both enthalpy changes and transition temperatures were determined using indium as the calibration standard. All of the samples were initially heated three times and cooled twice; their equilibrium transition temperatures and enthalpies were subsequently determined through extensive annealing and quenching studies. A Leica DMLP polarizing optical microscope

(magnification 200×) equipped with a Mettler FP82 hot stage and a Mettler FP90 central processor was used to observe the thermal transitions and to analyse the anisoptropic textures [11]. Thin samples were prepared by melting a minimum amount of compound between a clean glass slide and a cover slip, and rubbing the cover slip with a spatula.

The molecular modelling results were obtained using Cerius[2] Version 4.0 from Molecular Simulations Incorporated with the universal force field being used in all of the energy calculations. The energy minimization calculations were completed with the Smart Minimizer Method with the convergence criteria of RMS force of 0.1 kcal mol^{-1} $Å^{-1}$, energy difference of 1×10^{-3} kcal mol^{-1}, and RMS displacement of 3×10^{-3} Å. The volume of the lateral substituent was determined using the entire side chain (RCO_2CH_2-) plus hydrogen (RCO_2CH_3) in place of the mesogen. The energy of the structure was initially minimized, and then the total volume was calculated using the total free volume measurement in Cerius[2] and the fine grid spacing option.

The molecular dynamics trajectories were calculated using the laterally substituted mesogen, with $-OCH_3$ in place of the $-O(CH_2)_8(CF_2)_7F$ terminal substituents (figure 3). The trajectories were 1.0 ns at 460 K, constant NVT, with a 0.5 fs timestep, and the data recorded every 100 fs. The torsion angles ϕ_1 and ϕ_2 in figure 3 were monitored during the trajectories. Energy minimization was used to optimize the structures before the molecular dynamics trajectories were run. The autocorrelation function, $\langle \cos(\phi_{t+t^o} - \phi_{t^o}) \rangle$, was calculated to validate that 1.0 ns trajectories were long enough for the system to sample all of the accessible conformations.

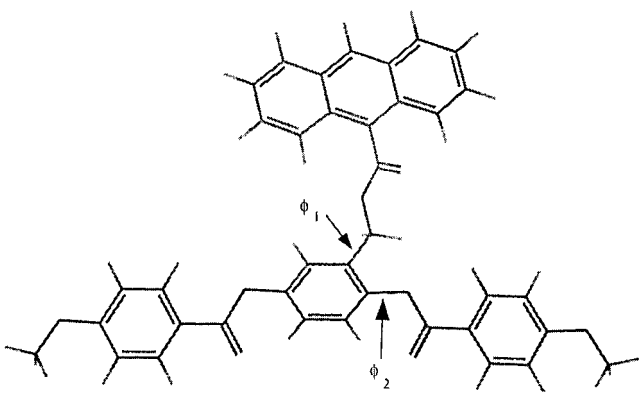

Figure 3. Example of a laterally substituted mesogen used in the molecular dynamics simulations.

A 'packing efficiency' value was used to determine how effectively two molecules could pack in the crystal. First, one of the most probable conformations for the structure was chosen from the molecular dynamics trajectory. Next, a copy of the structure was rotated 180° and placed above the original structure with the mesogens aligned parallel to each other and the lateral substituents in the middle (figure 4). The best packing of the two structures was found by energy minimization from numerous starting positions of the structures. Next, using the free volume measurement in Cerius[2], the surface area and volume were calculated using the accessible volume option with a 1.4 Å probe. From the surface area and volume measurements, a dimensionless packing efficiency, $1/E$, was calculated according to the following equation:

$$\frac{1}{E} = \frac{surface\ area}{4\pi(3V/4\pi)^{2/3}}.$$

As the value of this number increases from one, the packing becomes less efficient.

2.3. *Synthesis*

2.3.1. *Potassium alkanoates and benzoates*

The potassium alkanoates and benzoates were prepared in 78–100% yield as in the following example. A solution of 4-*t*-butylbenzoic acid (0.24 g, 1.3 mmol) in methanol (5 ml) was titrated to a phenolphthalein endpoint with 1.5M methanolic KOH (0.9 ml). The solution was concentrated to a slurry using a rotary evaporator, and then poured into cold diethyl ether (150 ml). The resulting precipitate was collected and dried to yield 0.22 g (78%) of potassium 4-*t*-butylbenzoate as a white, hygroscopic solid; m.p. >275°C.

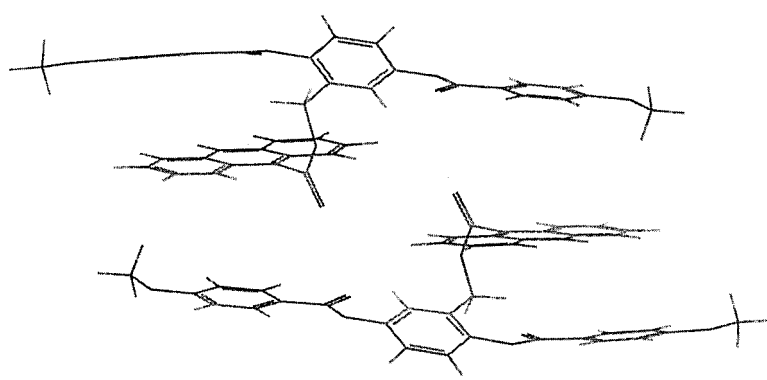

Figure 4. Starting position of two laterally substituted mesogens used to determine their packing efficiency.

2.3.2. *2,5-Bis[4-(n-perfluoroheptyloctyloxy)benzoyloxy]-benzyl alkanoates and benzoates*

These were prepared in 28–67% yield as in the following example. A solution of 2,5-bis[4-(*n*-perfluoroheptyloctyloxy)benzoyloxy]benzyl bromide (0.25 g, 0.14 mmol $ArCH_2Br$), potassium 1-adamantanecarboxylate (62 mg, 0.28 mmol), and TBAH (24 mg, 6.9 μmol) in THF (0.4 ml) and DMSO (40 μl) was heated at 60°C for 19 h. The reaction mixture was poured into cold water (125 ml). The resulting precipitate was collected, air dried for 1 h, and passed through a short column of basic activated alumina using CH_2Cl_2 as the eluant. The solvent was removed using a rotary evaporator to yield 0.19 g (88%) of a light orange solid. This crude product was purified by column chromatography using silica gel as the stationary phase and a gradient of CH_2Cl_2/hexanes as the eluant. The solvent was removed using a rotary evaporator, and the product was recrystallized from a mixture of ethanol (16 ml) and toluene (6 ml) to yield 0.094 g (45%) of 2,5-bis[4-(*n*-perfluoroheptyloctyloxy)-benzoyloxy]benzyl 1-adamantanecarboxylate as a white powder. ^{1}H NMR: 1.40 (m, $(CH_2)_3CH_2CH_2CF_2$, 12 H), 1.50 (m, $CH_2CH_2CH_2O$, 4 H), 1.62 (m, $CH_2CH_2CF_2$, 4 H), 1.66 (m, adamantyl C4H_2, C6H_2 & C10H_2), 1.80 (d, adamantyl C2H_2, C8H_2 & C9H_2), 1.83 (m, CH_2CH_2O, 4 H), 1.95 (s, adamantyl C3*H*, C5*H* & C7*H*), 2.05 (m, CH_2CF_2, 4 H), 4.05 (t, OCH_2, 4 H), 5.10 (s, $ArCH_2$), 6.98 (dd, 4 aromatic H *ortho* to OCH_2), 7.24 (dd, 1 aromatic H *para* to CH_2), 7.30 (d, 1 aromatic H *meta* to CH_2), 7.31 (d, 1 aromatic H *ortho* to CH_2), 8.14 (dd, 4 aromatic H *ortho* to CO_2Ar). Anal. ($C_{62}H_{60}F_{30}O_8$) C,H: calcd 49.54, 4.02; found 49.22, 4.26%.

2,5-Bis[4-(*n*-perfluoroheptyloctyloxy)benzoyloxy]-benzyl 9-anthracenecarboxylate. ^{1}H NMR: 1.39 (m, $(CH_2)_3CH_2CH_2CF_2$, 12 H), 1.49 (m, $CH_2CH_2CH_2O$, 4 H), 1.61 (m, $CH_2CH_2CF_2$, 4 H), 1.82 (m, CH_2CH_2O, 4 H), 2.06 (m, CH_2CF_2, 4 H), 4.03 (m, OCH_2, 4 H), 5.68 (s, $ArCH_2$), 6.93 (dd, 4 aromatic H *ortho* to OCH_2), 7.27 (dd, 1 aromatic H *para* to CH_2), 7.35 (d, 1 aromatic H *meta* to CH_2), 7.36 (d, 1 aromatic H *ortho* to CH_2), 7.45 (m, 4 aromatic H of anthracene at C2, C3, C6 & C7), 7.98 (m, 4 aromatic H of anthracene at C1, C4, C5 & C8), 8.11 (dd, 4 aromatic H *ortho* to CO_2Ar), 8.51 (s, 1 aromatic H of anthracene at C10). Anal. ($C_{66}H_{54}F_{30}O_8$) C,H: calcd 51.31, 3.52; found 51.22, 3.67%.

2,5-Bis[4-(*n*-perfluoroheptyloctyloxy)benzoyloxy]-benzyl benzoate. ^{1}H NMR: 1.39 (m, $(CH_2)_3CH_2CH_2CF_2$, 12 H), 1.49 (m, $CH_2CH_2CH_2O$, 4 H), 1.62 (m, $CH_2CH_2CF_2$, 4 H), 1.83 (m, CH_2CH_2O, 4 H), 2.06 (m, CH_2CF_2, 4 H), 4.04 (dt, OCH_2, 4 H), 5.38 (s, $ArCH_2$), 6.95 (dd, 4 aromatic H *ortho* to OCH_2), 7.27 (dd, 1 aromatic H *para* to CH_2), 7.32 (d, 1 aromatic H *meta* to CH_2), 7.39 (t, 2 aromatic H *meta* to CO_2CH_2), 7.42 (d, 1 aromatic H *ortho* to CH_2), 7.53 (t, 1 aromatic H *para* to CO_2CH_2), 7.98 (d, 2 aromatic H *ortho* to CO_2CH_2), 8.12 (dd, 4 aromatic H *ortho* to CO_2Ar). Anal. ($C_{58}H_{50}F_{30}O_8$) C,H: calcd. 48.21, 3.49; found 47.85, 3.52%.

2,5-Bis[4-(*n*-perfluoroheptyloctyloxy)benzoyloxy]-benzyl 2-biphenylcarboxylate. ^{1}H NMR: 1.40 (m, $(CH_2)_3CH_2CH_2CF_2$, 12 H), 1.51 (m, $CH_2CH_2CH_2O$, 4 H), 1.62 (m, $CH_2CH_2CF_2$, 4 H), 1.84 (m, CH_2CH_2O, 4 H), 2.06 (m, CH_2CF_2, 4 H), 4.06 (dt, OCH_2, 4 H), 5.11 (s, $ArCH_2$), 6.66 (d, 1 aromatic H *ortho* to CH_2), 6.98 (dd, 4 aromatic H *ortho* to OCH_2), (dd, 1 aromatic H *para* to CH_2), 7.21 (d, 1 aromatic H *meta* to CH_2), 7.24 (m, 5 aromatic H of Ph), 7.33 (d, 1 aromatic H *ortho* to Ph), 7.38 (t, 1 aromatic H *para* to Ph), 7.51 (t, 1 aromatic H *para* to CO_2CH_2), 7.81 (d, 1 aromatic H *ortho* to CO_2CH_2), 8.14 (dd, 4 aromatic H *ortho* to CO_2Ar). Anal. ($C_{64}H_{54}F_{30}O_8$) C,H: calcd. 50.54, 3.58; found 50.05, 3.82%.

2,5-Bis[4-(*n*-perfluoroheptyloctyloxy)benzoyloxy]-benzyl 4-biphenylcarboxylate. ^{1}H NMR: 1.39 (m, $(CH_2)_3CH_2CH_2CF_2$, 12 H), 1.48 (m, $CH_2CH_2CH_2O$, 4 H), 1.62 (m, $CH_2CH_2CF_2$, 4 H), 1.82 (m, CH_2CH_2O, 4 H), 2.06 (m, CH_2CF_2, 4 H), 4.03 (dt, OCH_2, 4 H), 5.41 (s, $ArCH_2$), 6.95 (dd, 4 aromatic H *ortho* to OCH_2), 7.28 (dd, 1 aromatic H *para* to CH_2), 7.33 (d, 1 aromatic H *meta* to CH_2), 7.39 (d, 1 aromatic H *ortho* to CH_2), 7.46 (m, 3 aromatic H *ortho* & *para* to $ArCO_2CH_2$), 7.60 (d, 2 aromatic H *ortho* to $ArCO_2CH_2$ and 2 aromatic H *ortho* to Ph), 8.03 (d, 2 aromatic H *meta* to Ph), 8.13 (dd, 4 aromatic H *ortho* to CO_2Ar). Anal. ($C_{64}H_{54}F_{30}O_8$) C,H: calcd. 50.54, 3.58; found 50.07, 3.74%.

2,5-Bis[4-(*n*-perfluoroheptyloctyloxy)benzoyloxy]-benzyl 4-*t*-butylbenzoate. ^{1}H NMR: 1.31 (s, $C(CH_3)_3$), 1.39 (m, $(CH_2)_3CH_2CH_2CF_2$, 12 H), 1.48 (m, $CH_2CH_2CH_2O$, 4 H), 1.62 (m, $CH_2CH_2CF_2$, 4 H), 1.82 (m, CH_2CH_2O, 4 H), 2.07 (m, CH_2CF_2, 4 H), 4.04 (dt, OCH_2, 4 H), 5.37 (s, $ArCH_2$), 6.95 (dd, 4 aromatic H *ortho* to OCH_2), 7.28 (dd, 1 aromatic H *para* to CH_2), 7.30 (d, 1 aromatic H *meta* to CH_2), 7.39 (d, 1 aromatic H *ortho* to CH_2), 5.41 (2 aromatic H *ortho* to *t*-butyl), 7.91 (d, 2 aromatic H *meta* to *t*-butyl), 8.12 (dd, 4 aromatic H *ortho* to CO_2Ar). Anal. ($C_{62}H_{58}F_{30}O_8$) C,H: calcd. 49.61, 3.89; found 49.31, 4.06%.

2,5-Bis[4-(*n*-perfluoroheptyloctyloxy)benzoyloxy]-benzyl 3,5-di-*tert*-butylbenzoate. ^{1}H NMR: 1.30 (s, $C(CH_3)_3$, 18 H), 1.39 (m, $(CH_2)_3CH_2CH_2CF_2$, 12 H), 1.49 (m, $CH_2CH_2CH_2O$, 4 H), 1.62 (m, $CH_2CH_2CF_2$, 4 H), 1.82 (m, CH_2CH_2O, 4 H), 2.06 (m, CH_2CF_2, 4 H), 4.03 (dt, OCH_2, 4 H), 5.39 (s, $ArCH_2$), 6.94 (dd, 4 aromatic H *ortho* to OCH_2), 7.27 (dd, 1 aromatic H *para* to CH_2), 7.32 (d, 1 aromatic H *meta* to CH_2), 7.44 (d, 1 aromatic H *ortho* to CH_2), 7.58 (t, 1 aromatic H *para* to CO_2CH_2), 7.83 (d, 2 aromatic H *ortho* to

CO_2CH_2), 8.12 (dd, 4 aromatic H *ortho* to CO_2Ar). Anal. ($C_{66}H_{66}F_{30}O_8$) C,H: calcd. 50.91, 4.27; found 50.68, 4.36%.

2,5-Bis[4-(*n*-perfluoroheptyloctyloxy)benzoyloxy]-benzyl 2-ethylbutanoate. ^{1}H NMR: 0.80 (t, CH_3CH_2CH, 6 H), 1.39 (m, $(CH_2)_3CH_2CH_2CF_2$, 12 H), 1.48 (m, $CH_2CH_2CH_2O$ and CH_3CH_2, 8 H), 1.61 (m, $CH_2CH_2CF_2$, 4 H), 1.82 (m, CH_2CH_2O, 4 H), 2.07 (m, CH_2CF_2, 4 H), 2.19 (m, CH), 4.05 (t, OCH_2, 4 H), 5.13 (s, $ArCH_2$), 6.97 (dd, 4 aromatic H *ortho* to OCH_2), 7.24 (dd, 1 aromatic H *para* to CH_2), 7.29 (d, 1 aromatic H *meta* to CH_2), 7.34 (d, 1 aromatic H *ortho* to CH_2), 8.14 (dd, 4 aromatic H *ortho* to CO_2Ar). Anal. ($C_{57}H_{56}F_{30}O_8$) C,H: calcd. 47.58, 3.92; found 47.24, 3.98%.

2,5-Bis[4-(*n*-perfluoroheptyloctyloxy)benzoyloxy]-benzyl 4-hexadecyloxybenzoate. ^{1}H NMR: 0.87 (t, CH_3), 1.25 (m, $[CH_2]_{13}$), 1.40 (m, $(CH_2)_3CH_2CH_2CF_2$, 12 H), 1.49 (m, $CH_2CH_2CH_2O$, 4 H), 1.62 (m, $CH_2CH_2CF_2$, 4 H), 1.79 (m, CH_2CH_2O, 6 H), 2.07 (m, CH_2CF_2, 4 H), 3.97 (t, $OCH_2(CH_2)_{15}H$), 4.04 (m, $OCH_2(CH_2)_6CF_2$, 4 H), 5.35 (s, $ArCH_2$), 6.84 (d, 2 aromatic H *meta* to CO_2CH_2), 6.95 (dd, 4 aromatic H *ortho* to OCH_2), 7.27 (dd, 1 aromatic H *para* to CH_2), 7.30 (d, 1 aromatic H *meta* to CH_2), 7.41 (d, 1 aromatic H *ortho* to CH_2), 7.91 (d, 2 aromatic H *ortho* to CO_2CH_2), 8.13 (dd, 4 aromatic H *ortho* to CO_2Ar). Anal. ($C_{74}H_{82}F_{30}O_9$) C,H: calcd. 52.74, 4.90; found 52.66, 5.06%.

2,5-Bis[4-(*n*-perfluoroheptyloctyloxy)benzoyloxy]-benzyl 4-methoxybenzoate. ^{1}H NMR: 1.38 (m, $(CH_2)_3CH_2CH_2CF_2$, 12 H), 1.48 (m, $CH_2CH_2CH_2O$, 4 H), 1.61 (m, $CH_2CH_2CF_2$, 4 H), 1.82 (m, CH_2CH_2O, 4 H), 2.06 (m, CH_2CF_2, 4 H), 3.83 (s, OCH_3, 3 H), 4.03 (dt, OCH_2, 4 H), 5.34 (s, $ArCH_2$), 6.85 (d, 2 aromatic H *ortho* to OCH_3), 6.94 (dd, 4 aromatic H *ortho* to OCH_2), 7.25 (dd, 1 aromatic H *para* to CH_2), 7.30 (d, 1 aromatic H *meta* to CH_2), 7.40 (d, 1 aromatic H *ortho* to CH_2), 7.92

Table 1. Thermal transitions and thermodynamic parameters of 2,5-bis[4-(*n*-perfluoroheptyloctyloxy)benzoyloxy]benzyl carboxylates.[a]

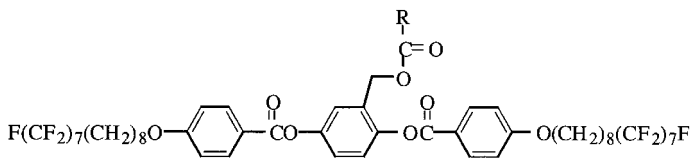

$R-CO_2-$	Volume of $R-CO_2CH_3$/Å^3	Phase transitions[a]/°C (ΔH/kJ mol^{-1}) Heating	Cooling
1-Adamantylcarboxylate	196.13	Cr 92 (28.2) [SmC 51[b]] SmA 154 (5.14) I	I 152 (5.24) SmA 52 (0.13) SmC 14 G
9-Anthracenecarboxylate[c]	218.24	G 24 SmC 60[b] SmA 219 (7.54) I	I 217 (7.77) SmA 56[b] SmC 21 G
Benzoate	130.44	Cr 85 (54.4) [SmC 72[b]] SmA 172 (7.62) I	I 170 (7.91) SmA 69[b] SmC 30 (35.3) Cr
2-Biphenylcarboxylate	204.06	Cr 100 (68.7) [SmC 40[b]] SmA 182 (7.30) I	I 179 (7.68) SmA 36[b] SmC 8 G
4-Biphenylcarboxylate	204.52	Cr 61 (27.9) SmC 76 (0.034) SmA 193 (6.90) I	I 190 (7.12) SmA 73 (0.563) SmC 13 G
4-*t*-Butylbenzoate	200.89	Cr 78 (43.7) SmC 85 (0.068) SmA 153 (5.25) I	I 150 (5.52) SmA 83 (0.177) SmC 10 G
3,5-Di-*t*-butylbenzoate	270.21	Cr 43 (21.3) [SmC 37 (0.033)] SmA 121 (4.61) I	I 117 (4.66) SmA 34 (0.079) SmC 9 G
2-Ethylbutanoate	147.83	Cr 73 (30.6) [SmC 73[b]] SmA 145 (7.02) I	I 142 (7.25) SmA 69[b] SmC 47 (26.3) Cr
4-Hexadecyloxybenzoate	350.73	Cr 82 (60.3) [SmC 60[b]] SmA 144 (5.57) I	I 141 (5.77) SmA 55 (0.054) SmC 40 (42.2) Cr
4-Methoxybenzoate	157.90	Cr 73 (41.8) [SmC 70[b]] SmA 182 (6.58) I	I 179 (6.82) SmA 68[b] SmC 25 (24.4) Cr
4-Octyloxybenzoate	207.45	Cr 75 (42.2) [SmC 83 (0.145)] SmA 159 (5.82) I	I 156 (6.32) SmA 80 (0.432) SmC 24 (14.7) Cr
2-Propylpentanoate	180.97	Cr 75 (63.2) [SmC 60[b]] SmA 141 (7.37) I	I 138 (7.56) SmA 57[b] SmC 21 (28.7) Cr

[a] G = glass, Cr = crystalline, SmC = smectic C, SmA = smectic A, I = isotropic, [] = monotropic. For comparison, 2,5-bis-[4′-(*n*-perfluoroheptyloctyloxy)benzoyloxy]toluene: Cr 120 (51.5) SmC 199 (0.75) SmA 200 (7.70) I [8].

[b] Transition detected only by POM.

[c] T_m of ethanol/toluene-crystallized sample = 113°C.

(d, 2 aromatic H *meta* to OCH_3), 8.12 (dd, 4 aromatic H *ortho* to CO_2Ar). Anal. ($C_{59}H_{52}F_{30}O_9$) C,H: calcd. 48.04, 3.55; found 47.76, 3.56%.

2,5-Bis[4-(*n*-perfluoroheptyloctyloxy)benzoyloxy]-benzyl 4-octyloxybenzoate. ^{1}H NMR: 0.88 (t, CH_3), 1.30 (m, $[CH_2]_5$), 1.39 (m, $(CH_2)_3CH_2CH_2CF_2$, 12 H), 1.49 (m, $CH_2CH_2CH_2O$, 4 H), 1.62 (m, $CH_2CH_2CF_2$, 4 H), 1.78 (m, CH_2CH_2O, 6 H), 2.06 (m, CH_2CF_2, 4 H), 3.98 (t, $OCH_2(CH_2)_7H$), 4.05 (dt, $OCH_2(CH_2)_6CF_2$, 4 H), 5.35 (s, $ArCH_2$), 6.84 (d, 2 aromatic H *meta* to CO_2CH_2), 6.95 (dd, 4 aromatic H *ortho* to OCH_2), 7.27 (dd, 1 aromatic H *para* to CH_2), 7.31 (d, 1 aromatic H *meta* to CH_2), 7.41 (d, 1 aromatic H *ortho* to CH_2), 7.92 (d, 2 aromatic H *ortho* to CO_2CH_2), 8.13 (dd, 4 aromatic H *ortho* to CO_2Ar). Anal. ($C_{66}H_{66}F_{30}O_9$) C,H: calcd. 50.39, 4.23; found 49.90, 4.40%.

2,5-Bis[4-(*n*-perfluoroheptyloctyloxy)benzoyloxy]-benzyl 2-propylpentanoate. ^{1}H NMR: 0.81 (t, CH_3, 6 H), 1.20 (m, CH_3CH_2, 4 H), 1.35 (m, $(CH_2)_3CH_2CH_2CF_2$ and $CH_2CH_2CH_3$, 16 H), 1.50 (m, $CH_2CH_2CH_2O$, 4 H), 1.62 (m, $CH_2CH_2CF_2$, 4 H), 1.82 (m, CH_2CH_2O, 4 H), 2.07 (m, CH_2CF_2, 4 H), 2.34 (m, CH), 4.05 (t, OCH_2, 4 H), 5.12 (s, $ArCH_2$), 6.97 (d, 4 aromatic H *ortho* to OCH_2), 7.24 (dd, 1 aromatic H *para* to CH_2), 7.29 (d, 1 aromatic H *meta* to CH_2), 7.32 (d, 1 aromatic H *ortho* to CH_2), 8.14 (d, 4 aromatic H *ortho* to CO_2Ar). Anal. ($C_{59}H_{60}F_{30}O_8$) C,H: calcd. 48.30, 4.12; found 47.86, 4.15%.

3. Results and discussion

As outlined in the scheme, the 2,5-bis[4-(*n*-perfluoroheptyloctyloxy)benzoyloxy]benzyl carboxylates were synthesized from 2,5-bis[4-(*n*-perfluoroheptyloctyloxy)-benzoyloxy]benzyl bromide [1, 8], by phase transfer

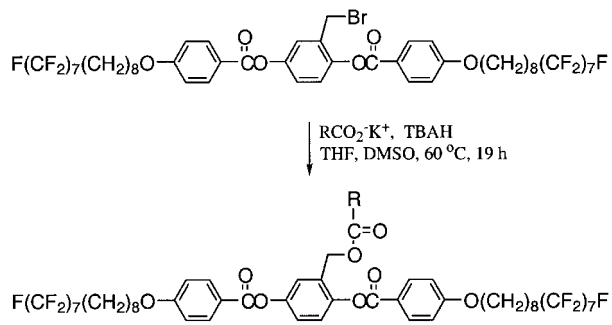

Scheme. Synthesis of 2,5-bis[4-(*n*-perfluoroheptyloctyloxy)-benzoyloxy]benzyl carboxylates.

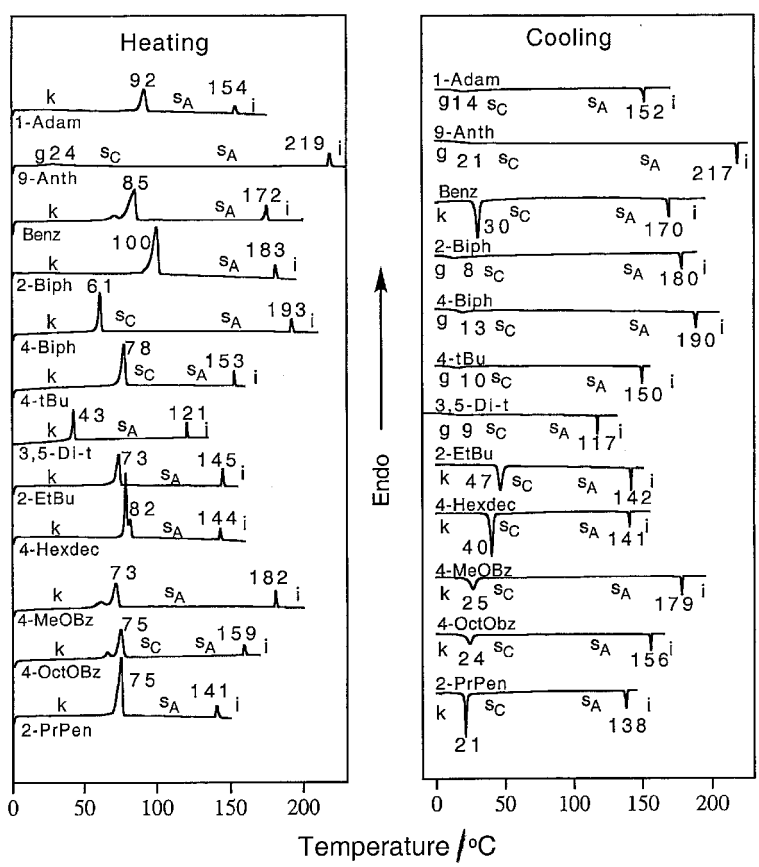

Figure 5. Normalized DSC traces of the 2,5-bis[4′-(*n*-perfluoroheptyloctyloxy)benzoyloxy]benzyl carboxylates observed on heating and on cooling at 10°C min^{-1}.

catalysed esterification with the corresponding potassium alkanoates and benzoates. The final yields of pure products were low because the products and unreacted benzyl bromide have similar R_f values, and therefore much of the product isolated by gradient chromatography is contaminated with unreacted starting material and/or side products.

Table 1 summarizes the thermotropic behaviour of the 2,5-bis[4-(*n*-perfluoroheptyloctyloxy)benzoyloxy]benzyl alkanoates and benzoates obtained on heating and cooling at 10°C min^{-1}. This data represents samples that were crystallized from solution and/or from the melt after annealing at room temperature for sufficient time to reach thermodynamic equilibrium. Figure 5 presents the corresponding DSC traces, which are normalized relative to each other. All of the compounds crystallize more slowly than the timescale of the DSC experiment. The 9-anthracenecarboxylate (T_m = 113°C from solution) does not recrystallize from the melt even after annealing for 7 months at room temperature. The 1-adamantylcarboxylate and 3,5-di-*t*-butylcarboxylate derivatives do not crystallize at all, on either cooling or reheating at 10°C min^{-1}, but do recrystallize after annealing at room temperature for a few months. The remaining compounds recrystallize at least partially on cooling and/or reheating, albeit to polymorphic structures with less thermodynamically stable crystalline phases; they recrystallize to the most thermodynamically stable phase only

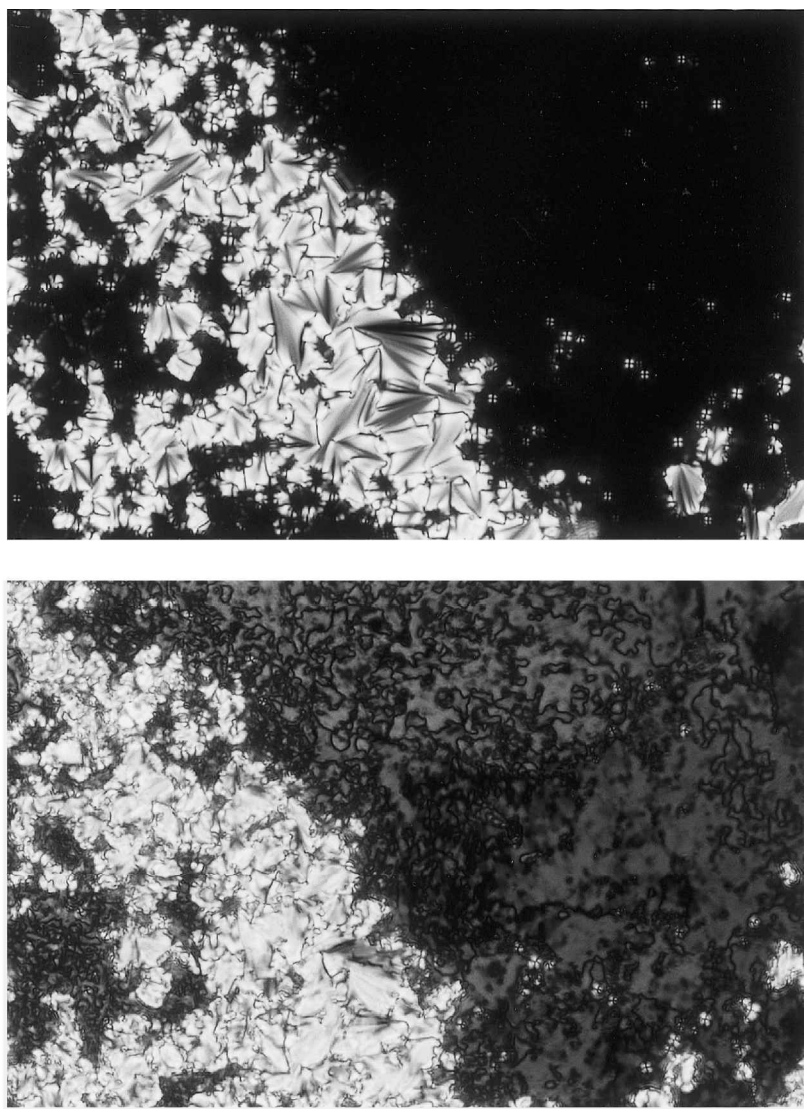

Figure 6. Polarizing optical micrographs (200×) observed on cooling 2,5-bis[4-(*n*-perfluoroheptyloctyloxy)benzoyloxy]benzyl 2-ethylbutanoate from the isotropic melt: (*a*) 132.7°C, SmA focal-conic fan and homeotropic textures; (*b*) 66.5°C, SmC broken focal-conic fan and schlieren textures.

after extensive annealing at room temperature plus 0.5–1 h annealing at elevated temperature. Some of these derivatives (4-*t*-butylbenzoate, 78 vs. 66°C; 4-methoxybenzoate, 73 vs. 68°C; 4-*n*-octyloxybenzoate, 75 vs. 65°C; and 2-propylpentanoate, 75 vs. 63°C) actually crystallize after annealing into a phase with a higher melting temperature than the solution-crystallized samples. Although most of the solution-crystallized samples have a single melting transition, it is often broad and encompasses two narrower transitions on subsequent scans. This indicates that the bulky lateral substituents of the 2,5-bis[4-(*n*-perfluoroheptyloctyloxy)benzoyloxy]benzyl carboxylates have two or more readily accessible conformations.

Although the bulky lateral substituents disrupt the ability of the 2,5-bis[4-(*n*-perfluoroheptyloctyloxy)-benzoyloxy]benzyl carboxylates to crystallize well, they do not convert the SmC and SmA mesophases of 2,5-bis-[4-(*n*-perfluoroheptyloctyloxy)benzoyloxy]toluene into a nematic mesophase. As shown by the representative polarizing optical micrographs in figure 6, the 2,5-bis-[4-(*n*-perfluoroheptyloctyloxy)benzoyloxy]benzyl carboxylates exhibit both natural textures of the SmA mesophase (homeotropic and focal-conic fan [11]), which convert to schlieren and broken focal-conic fan textures, respectively, upon cooling into the SmC mesophase. In contrast to the unsubstituted 2,5-bis[4-(*n*-perfluoroalkylalkoxy)benzoyloxy]toluenes which spontaneously macroscopically align in the SmA mesophase and exhibit a homeotropic texture [8], the focal-conic fan texture of these laterally substituted derivatives is initially easy to detect. However, the benzoate, 4-biphenyl carboxylate, 4-methoxybenzoate and 2-propylpentanoate derivatives slowly align to eventually exhibit primarily the homeotropic texture.

As mentioned in the introduction, the lateral *n*-alkanoyl substituents were not sufficiently bulky to disrupt the smectic layering of the 2,5-bis[4-(*n*-perfluoroheptyl-octyloxy)benzoyloxy]benzyl derivatives [1], although they did depress the melting, SmC–SmA, and isotropic transitions with increasing length of the *n*-alkanoyl substituent, until the transition temperatures leveled off to almost constant values at a length of six carbons (figure 2). All of the non-linear alkanoate and benzoate substituents studied here also depress both the melting and SmC–SmA transitions relative to unsubstituted 2,5-bis[4-(*n*-perfluoroheptyloctyloxy)benzoyloxy]toluene. Since these bulky substituents depress the temperature of the SmC–SmA transition more than that of melting, the SmC mesophase is either monotropic or exhibited over a much narrower temperature range relative to either 2,5-bis[4-(*n*-perfluoroheptyloctyl oxy)benzoyloxy]-toluene or the 2-*n*-alkyl-1,4-bis[4-(*n*-octyloxy)benzoyloxy]-benzenes, which have enantiotropic SmC mesophases.

With the exception of the 9-anthracenecarboxylate, all of the bulky lateral substituents also depress the SmA–I transition. Based on the inability of the 9-anthracene-carboxylate to recrystallize from the melt and the almost complete absence of homeotropic regions in its POM textures, the anthracene substituent seems to be the most disruptive of the substituents studied. The 1-adamantyl-carboxylate and 3,5-di-*t*-butylcarboxylate substituents are nearly as disruptive of crystallization since they exhibit only a glass transition on subsequent heating and cooling DSC scans at 10°C min^{-1}. As listed in table 1, these are also some of the bulkiest substituents. However, as shown in figure 7, there is no correlation between the temperature of any of the transitions and the volume of the lateral substituent. This is probably because the substituents vary from aromatic groups that could potentially interact with each other and with the aromatic rings of the mesogen through dipole–dipole interactions or by π-π stacking, to branched and cyclic aliphatic structures that can only interact with each other and the mesogen through van der Waals interactions.

We therefore performed molecular dynamics simulations of the 9-anthracenecarboxylate, 4-biphenyl-carboxylate, and 4-methoxybenzoate derivatives (which have the highest isotropization temperatures), 3,5-di-*t*-butylbenzoate (which has the lowest isotropization temperature), and the 1-adamantylcarboxylate (which has the only non-aromatic cyclic substituent), in order to understand better how these bulky lateral carboxyl substituents affect the packing of 2,5-bis[4-(*n*-perfluoro-heptyloctyloxy)benzoyloxy]benzyl derivatives. Figures 8(*a*) and 8(*b*) plot the torsion angles ϕ_1 and ϕ_2 (figure 3), respectively, as a function of time for the 9-anthracene-carboxylate derivative. It has four rotational states for

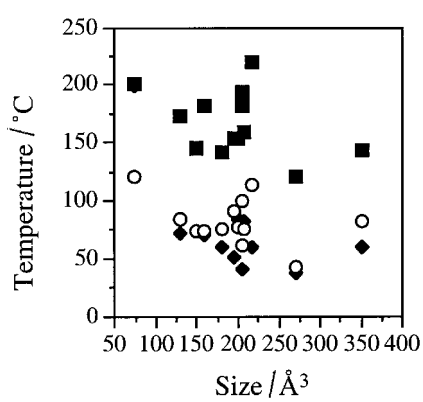

Figure 7. Dependence of the transition temperatures from the crystalline (○), smectic C (◆) and smectic A (■) phases of the 2,5-bis[4-(*n*-perfluoroheptyloctyloxy)benzoyloxy]-benzyl carboxylates as a function of the volume of the lateral substituent. The transition temperatures of the unsubstituted 2,5-bis[4-(*n*-perfluoroheptyloxtyloxy)benzoyloxy]-toluene [8] are shown at 73.08 Å^3 for comparison.

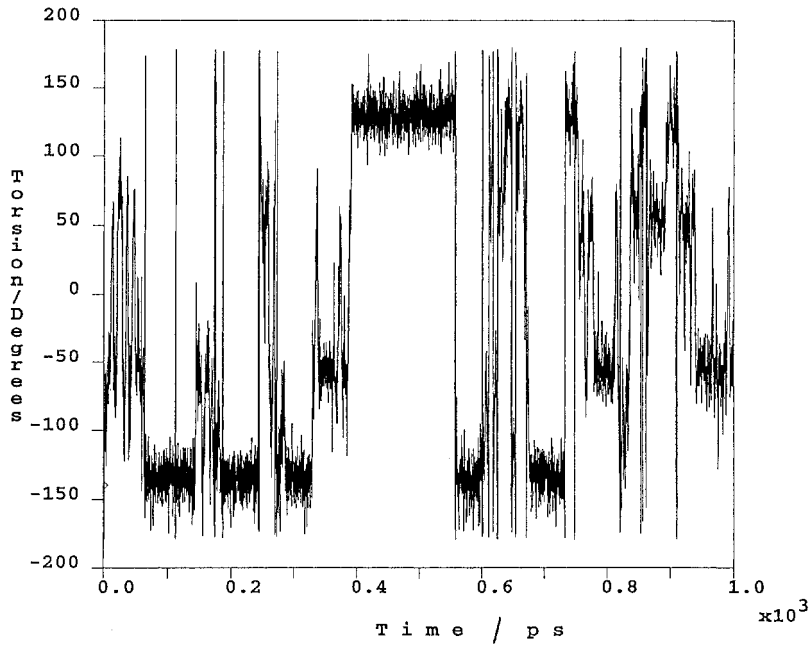

(*a*)

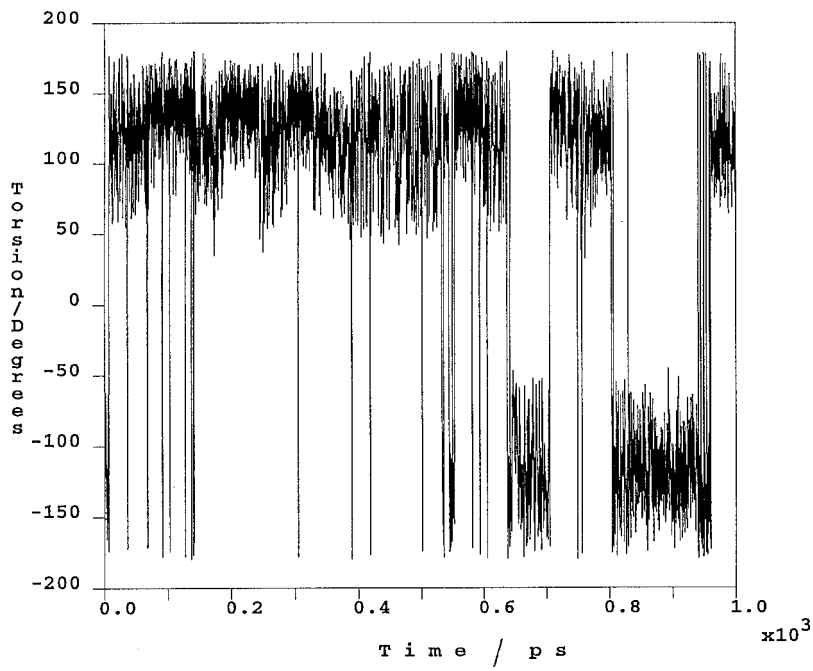

(*b*)

Figure 8. Torsion angle ϕ_1 (*a*) and ϕ_2 (*b*) plotted as a function of time from the molecular dynamics trajectory of 2,5-bis[4-(*n*-perfluoroheptyloctyloxy)benzoyloxy]benzyl 9-anthracenecarboxylate.

ϕ_1 (+/−60° and +/−130°), with +/−130° preferred. There are two rotational states for ϕ_2 (+/−125°). Table 2 lists the rotational states observed for ϕ_1 and ϕ_2 for the five simulated structures. Except for ϕ_1 of 9-anthracenecarboxylate, which has two additional rotational states for ϕ_1, all of the structures investigated have similar molecular dynamics trajectories. All of the structures, even those with the bulkiest substituents, rotate about ϕ_1 and ϕ_2. This evidently enables the bulky substituents to align parallel to the mesogen and pack efficiently.

Table 2. Rotational states for the torsion angles ϕ_1 and ϕ_2 and the packing efficiencies of two molecules of a sampling of 2,5-bis[4′-(*n*-perfluoroheptyloctyloxy)benzoyloxy]benzyl carboxylates.

R–CO_2–	ϕ_1	ϕ_2	Packing efficiency
1-Adamantylcarboxylate	+/−60°	+/−125°	1.64
9-Anthracenecarboxylate	+/−60°, +/−130°	+/−125°	1.47
4-Biphenylcarboxylate	+/−60°	+/−120°	1.58
3,5-Di-*t*-butylbenzoate	+/−60°	+/−125°	1.71
4-Methoxybenzoate	+/−60°	+/−120°	1.56

Figure 9 shows the best packing of two molecules of the 9-anthracenecarboxylate and 1-adamantylcarboxylate derivatives. This ability of the two molecules to pack was quantified using the packing efficiency value described in the experimental section and listed in table 2. Although the 9-anthracenecarboxylate substituent prevents crystallization of its derivative from the melt even after annealing for several months, it results in the highest SmA–I transition temperature (table 1), and therefore the most stable SmA mesophase. In addition, according to the packing efficiency values in table 2, its derivative packs the most efficiently of the five compounds studied by molecular simulations, followed by the 4-methoxycarboxylate and 4-biphenylcarboxylate derivatives. This demonstrates that a bulky lateral substituent can stabilize a smectic phase simultaneously with disrupting crystallization and destabilizing the crystalline phase.

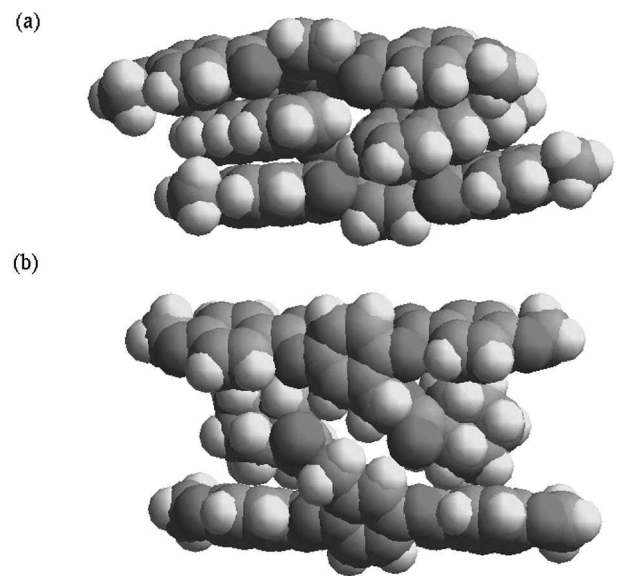

Figure 9. Best packing for two molecules of: (*a*) 2,5-bis[4-(*n*-perfluoroheptyloctyloxy)benzoyloxy]benzyl 9-anthracenecarboxylate; (*b*) 2,5-bis[4-(*n*-perfluoroheptyloctyloxy)-benzoyloxy]benzyl 1-adamantylcarboxylate.

As shown in figure 9, the two 9-anthracenecarboxylate derivatives are more densely packed than the two 1-adamantanecarboxylate derivatives; the mesogens are closer together and the two anthracene substituents completely fill the space between them. Surprisingly, the centres of mass of the two 9-anthracenecarboxylate derivatives are staggered, which corresponds to a tilted smectic phase (e.g. SmC), whereas the centres of mass of the 1-adamantanylcarboxylate derivatives are correlated, which corresponds to an orthogonal smectic phase (e.g. SmA). Although this indicates that the 1-adamantantylcarboxylate derivative might generate a more stable SmA mesophase compared with the 9-anthracenecarboxylate derivative, the two central aromatic rings of the stacked 1-adamantantylcarboxylate derivatives are not oriented so that they could readily interact with each other or the central aromatic rings of similar pairs by either dipole–dipole interactions or π-π stacking. The centres of mass of the two 4-biphenylcarboxylate and 3,5-di-*t*-butylcarboxylate derivatives are correlated; those of the two 4-methoxybenzoate derivatives are staggered.

4. Conclusions

Microsegregation of the hydrocarbon and fluorocarbon segments of 2,5-bis[4-(*n*-perfluoroheptyloctyloxy)-benzoyloxy]toluene is apparently so strong that bulky alkanoate and benzoate substituents do not disrupt smectic layering and convert the SmC and SmA mesophases into a nematic phase. However, most of the substituents studied were bulky enough to destabilize the SmC mesophase from an enantiotopic to a monotropic phase. Although the bulky 9-anthracenecarboxylate substituent was the most disruptive of crystallization, it resulted in the most stable SmA mesophase, which was consistent with the most densely packed structure according to molecular dynamics simulations. Based on molecular dynamics simulations of a sampling of the derivatives, all of the bulky substituents align parallel to the mesogen.

Acknowledgment is made to the donors of The Petroleum Research Fund, administered by the American Chemical Society, for support of this research. C.P. also acknowledges the National Science Foundation for an NSF Young Investigator Award (1994–2000), and matching funds from Goodyear Tire & Rubber Company and A. Schulman, Inc. W.L.M. acknowledges support by National Science Foundation grant DMR 98-44069.

References

[1] Small, A. C., Hunt, D. K., and Pugh, C., 1999, *Liq. Cryst.*, **26,** 849.
[2] Reinitzer, F., 1888, *Monatsch Chem.*, **9,** 421.

[3] (*a*) DEMUS, D., HAUSER, A., ISENBERG, A., POHL, M., SELBMANN, C., WEISSFLOG, W., and WIECZOREK, S., 1985, *Cryst. Res. Technol.*, **20,** 1413; (*b*) DEMUS, D., DIELE, S., HAUSER, A., LATIF, I., SELEMANN, C., and WEISSFLOG, W., 1985, *Cryst. Res. Technol.*, **20,** 1547; (*c*) REIN, C., and DEMUS, D., 1993, *Liq. Cryst.*, **15,** 193.

[4] (*a*) DEMUS, D., and ZASCHKE, H., 1984, *Flussige Kristalle in Tabellen II* (Leipzig: VEB Deutscher Verlag); (*b*) GRAY, G. W., 1979, in *The Molecular Physics of Liquid Crystals*, edited by G. R. Luckhurst, and G. W. Gray (London: Academic Press), p. 1; (*c*) ISHIZUKA, H., NISHIYMA, I., and YOSHIZAWA, A., 1995, *Liq. Cryst.*, **18,** 775.

[5] (*a*) YOUNG, W. R., and GREEN, D. C., 1974, *Mol. Cryst. liq. Cryst.*, **26,** 7; (*b*) WEISSFLOG, W., SCHLICK, R., and DEMUS, D., 1981, *Z. Chem.*, **21,** 452; (*c*) WEISSFLOG, W., and DEMUS, D., 1985, *Mol. Cryst. liq. Cryst.*, **129,** 235; (*d*) WEISSFLOG, W., WIEGELEBEN, A., and DEMUS, D., 1985, *Mat. Chem. Phys.*, **12,** 461; (*e*) BALLAUFF, M., 1987, *Liq. Cryst.*, **2,** 519; (*f*) IMRIE, C. T., and TAYLOR, L., 1989, *Liq. Cryst.*, **6,** 1; (*g*) STÜTZER, C., WEISSFLOG, W., and STEGEMEYER, H., 1996, *Liq. Cryst.*, **21,** 557; (*h*) ANDERSCH, J., and TSCHIERSKE, C., 1996, *Liq. Cryst.*, **21,** 51.

[6] ARORA, S. L., FERGASON, J. L., and TAYLOR, T. R., 1970, *J. org. Chem.*, **35,** 4055.

[7] (*a*) WEISSFLOG, W., and DEMUS, D., 1983, *Cryst. Res. Technol.*, **18,** K21; (*b*) WEISSFLOG, W., and DEMUS, D., 1984, *Cryst. Res. Technol.*, **19,** 55.

[8] AREHART, S. V., and PUGH, C., 1997, *J. Am. chem. Soc.*, **119,** 3027.

[9] (*a*) DIELE, S., ROTH, K., and DEMUS, D., 1986, *Cryst. Res. Technol.*, **21,** 97; (*b*) DIELE, S., WEISSFLOG W., PELZL, G., MANKE, H., and DEMUS, D., 1986, *Liq. Cryst.*, **1,** 101; (*c*) PEREZ, F., BERDAGUE, P., JUDEINSTEIN, P., BAYLE, J. P., ALLOUCHI, H., CHASSEAU, D., COTRAIT, M., and LAFONTAINE, E., 1995, *Liq. Cryst.*, **19,** 345; (*d*) BERDAGUE, P., PEREZ, F., BAYLE, J. P., HO, M.-S., and FUNG, B. M., 1995, *New J. Chem.*, **19,** 383.

[10] PUGH, C., and SCHROCK, R. R., 1992, *Macromolecules*, **25,** 6592.

[11] (*a*) GRAY, G. W., and GOODBY, J. W., 1984, *Smectic Liquid Crystals. Textures and Structures* (Glasgow: Leonard Hall); (*b*) DEMUS, D., and RICHTER, L., 1978, *Textures of Liquid Crystals* (Weinheim: Verlag Chemie).